Trends in the Hydrologic Regime of Alpine Rivers

Antony Bard, Benjamin Renard, M. Lang, I. Giuntoli, J. Korck, G. Koboltschnig, M. Janza, M. d'Amico, D. Volken

Trends in the hydrologic regime of Alpine rivers

Bard, Antoine; Renard, Benjamin; Lang, Michel; Giuntoli, Ignazio; Korck, Jane; Koboltschnig, Gernot; Janža, Mitja; D'amico, Michele; Volken, David

DOI:
10.1016/j.jhydrol.2015.07.052

Accepted Manuscript

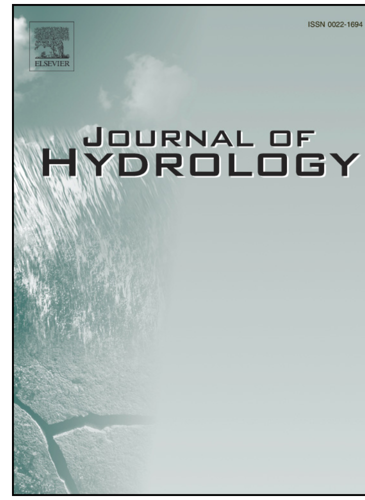

Trends in the Hydrologic Regime of Alpine Rivers

Antoine Bard, Benjamin Renard, Michel Lang, Ignazio Giuntoli, Jane Korck, Gernot Koboltschnig, Mitja Janža, Michele d'Amico, David Volken

PII: S0022-1694(15)00558-2
DOI: http://dx.doi.org/10.1016/j.jhydrol.2015.07.052
Reference: HYDROL 20618

To appear in: *Journal of Hydrology*

Received Date: 17 September 2013
Revised Date: 16 June 2015
Accepted Date: 29 July 2015

Please cite this article as: Bard, A., Renard, B., Lang, M., Giuntoli, I., Korck, J., Koboltschnig, G., Janža, M., d'Amico, M., Volken, D., Trends in the Hydrologic Regime of Alpine Rivers, *Journal of Hydrology* (2015), doi: http://dx.doi.org/10.1016/j.jhydrol.2015.07.052

Trends in the Hydrologic Regime of Alpine Rivers

Antoine Bard [1], *Benjamin Renard* [1], *Michel Lang* [1], *Ignazio Giuntoli* [1,2], *Jane Korck* [3],

Gernot Koboltschnig [4], *Mitja Janža* [5], *Michele d'Amico* [6], *David Volken* [7]

(1) Irstea, UR HHLY Hydrology-Hydraulics, Lyon, France.
(2) School of Geography, Earth & Environmental Sciences, University of Birmingham, Birmingham, United Kingdom.
(3) Bavarian Environment Agency, Hof, Germany.
(4) Dept. of Water Management, Provincial Government of Carinthia, Klagenfurt, Austria.
(5) Geological Survey of Slovenia, Ljubljana, Slovenia.
(6) Ministry for the Environment, Land and Sea, Italy.
(7) Federal Office for Environment, Bern, Switzerland.

Corresponding author:
Antoine Bard
+33 (0) 7 82 56 66 63
antoine.bard@hydro-consultant.com

Submitted for publication in Journal Of Hydrology

June 2015

Abstract

This paper describes a trend analysis performed on 177 streamflow time series collected over the Alps in Central Europe. The analysis covers several facets of the Alpine hydrologic regimes, including winter droughts and spring snowmelt flows, both in terms of severity and timing of occurrence. Statistical trend tests are applied at a local scale (i.e. on a site-by-site basis) and at a regional scale (seeking a common trend for sites within the same hydro-climatic region). The overall results indicate a trend toward less severe winter droughts, and consistent changes in the timing of snowmelt flows. However, a more in-depth analysis at the scale of hydro-climatic regimes reveals more contrasted changes. While most glacial- and snowmelt-dominated regimes show a decreasing trend in the severity of winter droughts, contrasted trends are found for mixed snowmelt-rainfall regimes in the Southeastern Alps. Changes in the timing of snowmelt flows (earlier start and increased duration of the snowmelt season) mostly affect glacial- and snowmelt-dominated regimes. Lastly, glacial regimes show an increase in the volume and the peak of snowmelt flows.

Keywords: Streamflow, Trend analysis, Alps, Snowmelt, Droughts, Spring onset.

Introduction

1.1. Detecting trends in hydrologic series

Trend analyses have received widespread attention in the hydrologic and climate communities (see e.g. Kundzewicz *et al*., 2005; Moberg and Jones, 2005; Svensson *et al.*, 2005; Pujol *et al.*, 2007; Hannaford and Marsh, 2008; Stahl *et al.*, 2010; Hodgkins and Dudley, 2011; Giuntoli *et al.*, 2013 for recent examples). Trend analysis is indeed a useful preliminary step to assess the existence of significant changes in hydro-climatic series, before attempting to understand their possible causes (Merz *et al.*, 2012). The detection of trends within hydrologic series raises several challenges. Firstly, the inter-annual variability of hydrologic series is generally very large, especially in the extreme domain, hence restricting the power of statistical tests to detect trends based on relatively short series. Secondly, many catchments are impacted by direct anthropogenic influences, such as water withdrawal or hydro-electricity production, which may create artificial trends in addition to climate trends. Lastly, ensuring the homogeneity of streamflow measurements over several decades is difficult: rating curves may change or gauging stations may be relocated, thus creating spurious trends in the time series (Lang *et al.*, 2010). Specific testing procedures (Kundzewicz and Robson, 2000; Parey *et al.*, 2007; Renard *et al.*, 2008) and thoroughly-reviewed datasets of undisturbed catchments (Hannah *et al.*, 2011; Burn *et al.*, 2012; Whitfield *et al.*, 2012) are required to face these challenges.

1.2. Observed trends in hydro-climatic variables in the Alps

Many studies have investigated the existence of trends in cryospheric variables over the world. Chapter 4 of the IPCC report (2013) provides an overview of these studies. We focus here on reviewing trend analyses for hydro-climatic variables in the Alpine region.

Stewart (2009) presents an overview of the changes in snowpack and snowmelt-related flows in the Alps and in other mountainous areas of the world. Focusing on the Alps, an overall decrease in snow cover is observed during the 20th century for low- and mid-elevations. Trends are less significant at higher elevations, and snowpack even increased due to higher precipitation totals. Auer *et al.* (2007) and Brunetti *et al.* (2006; 2009) describe an analysis of several climate variables over the Alpine region based on the HISTALP dataset. A general increase in annual temperature and air pressure is observed during the 20th century. Trends in precipitation are spatially more variable: for instance, annual totals increase in the northwest but decrease in the southeast. Other studies have focused on national scales and specific variables. In one such study, Frei and Schär (2001) analyzed 133 raingauges in Switzerland and found an increase in the frequency of intense events in winter and autumn during the 20th century.

Trend analyses on streamflow variables have often been performed at a relatively small spatial scale, for specific sub-regions within the Alpine area (see Viviroli *et al.*, 2011 for an overview). Birsan *et al.* (2005) analyzed 48 gauging stations in Switzerland, and found increases in winter, spring and autumn streamflow. Castellarin and Pistocchi (2012) used 17 stations in the Swiss Alps observing upward trends in annual streamflow maxima. In the French Alps, Giuntoli *et al.* (2012) observed decreasing high flow volumes from high-elevation catchments. In the same region, Renard *et al.* (2008) also observed an earlier timing of snowmelt-related flows, less severe winter droughts and an increase in annual flow for highly glacierized catchments. For the latter catchments, Pellicciotti *et al.* (2010) found similar results in Switzerland (see also Casassa *et al.*, 2009 for other mountainous areas of the world). The results for highly glacierized catchments seem consistent with what is expected in a warming climate, as described by Huss *et al.* (2008).

The study of Bard *et al.* (2012) is one of the few analyses covering the whole Alpine region for streamflow variables, but was restricted to high flows. Results showed an increase in the volume and peak of snowmelt flow for glacial regimes, and an earlier start of snowmelt flow. Lastly, the European-wide study of Stahl *et al.* (2010), based on 441 small undisturbed catchments, encompassed about 110 catchments in the Alpine region; trends toward less severe winter droughts were detected in most of them.

1.3. Objectives

The objective of this paper is to assess the existence of trends affecting hydrologic regimes in the Alps. The analysis described herein is unique in several respects. Firstly, it uses an extended and thoroughly-reviewed dataset of daily streamflow series covering most of the Alpine region. Secondly, it uses hydrologic indices adapted to the peculiarities of snowmelt-influenced catchments, and describing low, medium and high flows. Lastly, it operates at both local and regional scales, enabling a comprehensive assessment of the detected trends consistency.

The paper is organized as follows. Section 2 describes the dataset of daily streamflow series and its properties. Section 3 describes the methods used to analyze the evolution of hydrologic regimes, and more precisely the definition of hydrologic indices and the statistical setup for trend detection. The results are presented in Section 4 and discussed in Section 5. In Section 6 the main outcomes of this work are summarized.

2. The AdaptAlp Dataset

2.1. Daily streamflow series and associated catchments

The dataset used in this paper was gathered within the EU Alpine Space Programme project AdaptAlp, and is therefore named after it. The AdaptAlp dataset contains daily streamflow series for snowmelt-influenced catchments located in the Alps. As described in Bard *et al.* (2012), the strategy used to gather these series involves extensive quality checks in order to meet the following requirements: (a) the gauging station has been active over a period of at least 40 years; (b) the station controls a largely "undisturbed" catchment where direct anthropogenic influences can be neglected; (c) the daily streamflow series is free from any major non-homogeneity due to measurement issues.

Data quality has been assessed through a first round of analysis investigating changes affecting low, medium and high flows over the whole available period for each gauging station. In particular, step-change tests (Pettitt 1979) were used to highlight suspicious stations. For example a significant step change occurring on the same date for many hydrologic indices may be indicative of a measurement inhomogeneity (e.g. due to station relocation, change in the measurement sensor or method, etc.). The results from this first round of analysis were discussed with the data producers. Following this discussion, stations were excluded from the dataset whenever a specific cause for the detected change could be identified (typically, station relocation, building of some hydraulic structure influencing the river flow, etc.). Some of the stations were judged appropriate only for a specific flow range. As an example, some stations are only usable for high flow analyses because measurement issues and/or minor direct influences compromise their suitability for low flows.

This selection strategy yields a total of 177 series from six countries[1] (Austria, France, Germany, Italy, Slovenia and Switzerland, see Fig. 1a). Amongst these 177 series, 140 are suitable for high flow analyses, 134 for low flow analyses and 126 for all flow ranges. Figure 1b shows the effective record length (i.e. after the removal of missing values), with most stations providing between 40 and 50 years of daily data. A few series are effectively shorter than 40 years (due to missing data), while a few others are very long, with more than

[1] The names of the 177 gauging stations are given in the online material.

80 years of data. Note that the series may appear quite short compared to other meteorological variables. For instance, in the HISTALP project (Auer *et al.*, 2007), many series span the whole 20th century for variables such as air pressure, temperature or precipitation. Such long series are unfortunately scarcely available for streamflow data: while long series of water stages do exist, the same is not true for rating curves that estimate the stage-discharge relationship, thereby reducing the availability of reliable streamflow data. At the time of writing of this paper, 169 time series from the Adaptalp dataset have been made available through the Global Runoff Database Center[2].

The station elevations range mostly between 400 and 1200 m.a.s.l. (Fig. 1c). The dataset comprises catchments of varied size, the majority of which have an area between 100 and 1000 km² (Fig. 1d). Around twenty catchments have a significant part of their area covered by glacier, however precise quantification was not available for all of them. Lastly, Figure 1f shows the data availability, and suggests that the period 1961-2005 provides the best trade-off for analyzing as many stations as possible over a 40 years long common period.

2.2. Hydrologic regimes and hydro-climatic regions

Although all catchments in the AdaptAlp dataset are influenced by snowmelt, they still span a significant diversity of hydrologic regimes. The catchments are clustered into homogeneous hydrologic regimes to allow regime-specific analyses. Nine regimes are defined as presented in Figure 2; they range from pure glacial and snowmelt regimes to mixed snowmelt-rainfall regimes. The regimes clustering is performed by applying the Kohonen algorithm (Wehrens and Buydens, 2007) to the inter-annual monthly streamflow (standardized by the inter-annual mean) computed for each station. The Kohonen algorithm was chosen because it imposes

[2](GRDC: http://www.bafg.de/GRDC/EN/Home/homepage_node.html)

continuity between clusters, thus mimicking the continuous shift from glacial regimes to mixed snowmelt-rainfall regimes. Loosely speaking, hydrologic regimes are hence sorted by decreasing values of the annual solid/liquid precipitation ratio. Also note that the naming of each hydrologic regime is based on the interpretation of each cluster rather than on a detailed analysis of the dominant flow processes: this may not suffice to distinguish between e.g. glacial melt and snowmelt from high-elevation regions (Koboltschnig and Schoner, 2011).

As seen in Figure 3 pure glacial- and snowmelt-dominated regimes are found in the heart of the Alps. These hydrologic regimes are mainly controlled by the storage of precipitation as snow and ice during the cold months, with the lowest flows occurring between December and February (see Fig. 2). While the highest flows occur during spring and summer. The month with the highest flow ranges between April for composite 1 regimes to July for glacial regimes, owing to snow and ice melt and summer precipitation (Birsan *et al.*, 2005). On the other hand, mixed snowmelt-rainfall regimes are found in pre-alpine regions and behave differently, exhibiting two low flow seasons: during the winter when part of the precipitation is stored as snowpack, and during the summer due to a combination of earlier snowpack shortage, lack of precipitation and high evapotranspiration. For these regimes, high flows are mainly driven by snowmelt during the spring and by abundant precipitation in autumn.

Similarly to the hydrologic regimes, the Alpine area also spans a diversity of climatic regions. The four climatic regions defined in the HISTALP project (Auer *et al.*, 2007) are used (Fig. 3). This classification is based on climatic variables including normalized air pressure, air temperature, precipitation, cloudiness, and sunshine duration.

The climatic and hydrologic classifications are complementary because the former creates homogenous regions based on the main climate forcing, while the latter ensures the homogeneity of the hydrologic regimes at the catchment scale. Therefore, both classifications are combined to create homogeneous hydro-climatic regions, grouping catchments with similar hydrologic behavior and forced by similar climatic drivers.

3. Methods

3.1. Streamflow indices

The present study focuses on specific properties of Alpine rivers like winter low flows or spring and summer snowmelt-induced high flows. This is achieved by defining several hydrologic indices that are described in this section.

3.1.1. Flow duration curve percentiles

The first group of indices is obtained by using percentiles *Qx* of the annual flow duration curve, with *x* = 10%, 25%, 50%, 75%, 90% and 100%. This approach was used in a similar analysis by Lins and Slack (1999) and Birsan *et al.* (2005). It has the advantage of describing the whole spectrum of flows observed each year, by using an ensemble of percentages *x* between 10 and 100. For these indices, we use the 126 stations that are suitable for all flow ranges.

3.1.2. Winter low flows

Low flows are defined using a threshold approach (e.g. Fleig *et al.*, 2006): a low-flow threshold that equals the 15% percentile of the inter-annual flow duration curve is computed for each station. Three indices describing the drought severity are then defined as illustrated in Figure 4a: the volume deficit, the drought duration and the minimum streamflow (*Amin*). The volume deficit is calculated as the cumulative difference between the actual flow and the low flow threshold. In addition, three timing indices describing the drought timing are calculated: the drought “start” is defined as the date at which the cumulated volume deficit reaches 10% of the total volume deficit. Similarly, the drought “center” and the drought “end” correspond to 50% and 90% of the total volume deficit. These timing indices are similar to the "center of mass" defined by Stewart *et al.* (2005). For these indices, we use the 134 stations that are suitable for low flows.

3.1.3. Spring and summer high flows

In order to focus on snowmelt-related streamflow occurring during spring and summer, the daily time series are filtered to remove isolated rainfall-induced peaks: this is achieved using the base flow separation (BFS) method proposed by Tallaksen and Van Lanen (2004). A similar filtering was also used by Hodgkins and Dudley (2011) for base flow trend detection. Given the alpine character of the studied catchments, the filtered series is interpreted as snowmelt-induced base flow. Six indices are then extracted from the filtered series (Fig. 4b). The base flow maximum (*Amax*) and volume describe the snowmelt intensity. Similarly, as in section 3.1.2, high flow timing is described with the indices "start", "center" and "end", defined as the dates at which 10%, 50% and 90% of the base flow volume is reached. Lastly, the time between the snowmelt "start" and "end" gives an indication on the duration of the snowmelt-induced flows. For these indices, we use the 140 stations that are suitable for high flows.

3.1.4. Calculation time windows

The extraction of all hydrologic indices defined in sections 3.1.1-3.1.3 is not based on calendar years (from 1st of January to 31st of December) but on selected time windows which depend on the target index and hydrologic regime. Table 1 summarizes the time windows chosen in this study. Time windows are based on the annual regime shown in Figure 2: for high flow indices, the time window starts and ends on the months with the smallest streamflow (and *vice versa* for low flow indices). Consequently, calculation time windows are centered on the spring-summer runoff peak for high flows and on the coldest period for low flows.

3.1.5. Remark on timing indices

The timing of snowmelt flow is an important property of Alpine catchments, and it has been studied by several authors (Stewart *et al.* 2005). However, the use of “center of mass” or “center of volume” indices has been criticized by Dery *et al.* (2009) and Whitfield (2013). This metric is sensitive to the runoff volume variation and to the choice of calculation time window. It is also unable to capture changes associated with two or more dominant flow components. In the context of this paper, it is worth making a few considerations on the limitations of timing indices. First of all, our stations are strongly driven by snowmelt. For all regime types, snowmelt-induced volume contributes to most of the annual runoff volume, even for mixed snowmelt-rainfall regimes where the snowmelt induced runoff is still more important or is fairly equivalent to the runoff produced by autumnal precipitation (Fig. 2). Secondly, calculation time windows are specific to the target streamflow index and are centered either on the low or high flow period. Lastly, for high flows the base flow separation method is used in order to remove runoff induced by rainfall events and to only consider snowmelt-induced base flow.

3.2. Statistical tests

Trend detection is performed by applying statistical tests to the time series of hydrologic indices defined in the previous section 3.1. All testing procedures are detailed in Appendix 1.

3.2.1. At-site tests

The Mann-Kendall trend test (Mann, 1945; Kendall, 1975) is used for at-site trend detection. This test was selected because it is distribution-free, i.e. it does not require making any distributional assumption. However, this test does assume data independence, which may not be the case for some of the indices used in this study (especially low-flow indices). Therefore, the “modified” Mann-Kendall (MMK) test proposed by Hamed and Rao (1998) is implemented. We favored this test over possible alternatives such as prewhitening (see e.g. Von Storch and Navarra 1999) because Monte Carlo experiments (not detailed here) suggested that the MMK test performs at least equally well in general, and is even more powerful in some cases (e.g. strong autocorrelation, Renard 2006).

3.2.2. Field significance

When applying a statistical test to a large number of series with a 10% error level, a detection rate of about 10% of significant trends is expected, even in absence of any change in the series. Therefore, at-site testing is complemented by an evaluation of field significance, which answers the following question: what is the minimum number of significant at-site trends ensuring that these trends are not due to chance? The Bootstrap procedure proposed by Douglas *et al.* (2000), specifically designed to account for the spatial correlation within a dataset, is used for this purpose. Field significance is evaluated for each hydrologic regime, and for the whole dataset.

3.2.3. Regional consistency

Although an assessment of field significance is necessary to qualify detected trends at a regional level, it does not allow evaluating the trends consistency within a homogenous hydro-climatic region. As an illustration, a region affected by numerous trends both in upward and downward directions can be “field significant” despite a lack of consistency in detected trends. However, in the context of climate-related trend detection, one would expect that catchments with similar behavior and located in the same climatic region will respond in a similar way to the evolution of climate forcings. Consequently, the trends consistency is studied by applying the regional test proposed by Renard *et al.* (2008) at the scale of the hydro-climatic regions defined in section 2.2. In a nutshell, this test attempts to detect a common trend for a set of stations located in the same hydro-climatic region. It is a stringent test since it requires consistency, and will therefore not detect strong at-site trends that are not consistent across the region. On the other hand, it is powerful for detecting small but consistent trends that would be otherwise missed by at-site tests.

4. Results

All tests described in section 3.2 are applied with an error level of 10%. At-site tests are applied to series restricted to the common period 1961-2005, leading to the analysis of 126 to 140 stations (depending on the stations quality for low, medium, or high flows). Field significance is then evaluated for all stations and for each hydrologic regime separately (see Table 2). Lastly, the period of study for the regional consistency test is region-specific in order to optimize the number of stations available for each hydro-climatic region. However, these periods broadly cover the same period 1961-2005. For a given station, years with a missing value rate exceeding 0.5% are excluded from the series.

Trend magnitudes are only presented for significant detections and are averaged either across all stations or by hydrologic regime type. They are computed with the formula proposed by Sen (1968). For indices representing a discharge or a volume metric, trends are normalized by the mean index value and are expressed as the total variation over the 1961-2005 period in percent. For timing indices, trends are expressed as absolute values, quantifying the change over the period 1961-2005 as a number of days.

While the results related to floods have already been presented by Bard *et al.* (2012), this paper provides a general overview of the trends detected on the three components of the hydrologic regime of alpine rivers: low, medium and high flows. An additional analysis based on a subset of 22 long series covering the period 1925-2005 is also presented in section 4.4.

4.1. Percentiles

Figure 5 maps the trends detected with the at-site test, while Figure 6 shows the result of the field significance evaluation (at the scale of hydrologic regimes) and of the regional consistency test (at the scale of hydro-climatic regions). Note that there are very few Italian stations in Figure 5: this is due to extended periods of missing values in the 1980s, corresponding to a reorganization of the hydrological services. By restricting the analysis to the common period 1961-2005, those stations could not be considered in the analysis. However, Italian stations are included in the regional analysis (Fig. 6, mostly in the southwest climatic region), as region-specific periods allow for more flexibility in the station selection.

4.1.1. Lower percentiles (Q10, Q25)

Figure 5 shows a general increase in lower percentiles Q10 and Q25, with averaged trend magnitudes of 11% and 12% for all stations. This increase is particularly noticeable for glacial-influenced regimes (Table 2), with more than 60% of significant upward trends, and trend magnitudes of 26% and 31%. This increase holds to a lesser extent for snowmelt and composite regimes. The increasing trend is generally consistent at the scale of hydro-climatic regions (Fig. 6), especially in the northwest region. However, mixed snowmelt-rainfall regimes show the opposite behavior, with decreasing lower percentiles, especially in the southeast region.

4.1.2. Annual Median flow (Q50)

The annual median flow shows no clear general behavior over the whole Alpine region (Fig. 5). However, a clear increase appears for glacial regimes (Table 2), with 77% of significant upward trends and a trend magnitude of 36%. This increase is also found at the regional scale for snowmelt 1 regimes in both western regions (Fig. 6), but it is not field-significant (only 13% of at-site significant trends). Lastly, for composite 2 and snowmelt-rainfall 2 regimes the annual median flow is significantly decreasing with trend magnitudes of respectively 1% and 16%, but the regional consistency tests are not significant.

4.1.3. Higher percentiles (Q75, Q90, Q100)

Results for the higher percentiles are broadly similar to those of the annual median flow: no clear change appears over the Alps (Fig. 5), but some changes are field significant or regionally consistent at a smaller scale. In particular, upper percentiles increase for glacial regimes with moderate trend magnitudes of 17% and 15% (Table 2 and Fig. 6). Conversely, upper percentiles decrease for snowmelt-rainfall 1 and snowmelt-rainfall 2 regimes with trend magnitudes of 28% and 15% respectively.

4.2. Winter low flows

The low flow indices complete the description provided by the lower percentiles of section 4.1.1, with a characterization of winter low flows more focused on drought events. Results for low flows are presented similarly to section 4.1: in Figure 7 the trends detected with the at-site test are mapped with numbers provided in Table 2. Figure 8 shows the evaluation of field significance and regional consistency.

4.2.1. Severity

Winter drought severity appears to decrease overall (Fig. 7a-c): volume deficit (a) is indeed significantly decreasing for 25% of stations (Table 2), with a trend magnitude of 39% and drought duration (c) for 26% of stations with a reduction of 21 days on average. Annual minimum (b) is significantly increasing for 25% of stations with a trend magnitude of 16%

overall. These results are expressed in Figure 8 at the scale of the hydro-climatic regions: glacial, snowmelt-glacial and snowmelt 1 and 2 regimes present a clear signal toward less severe droughts: decrease in the drought duration and volume deficit and rise of the minimum streamflow value. This signal is reinforced by regionally significant trends in both western regions. Trend magnitudes are important for all regimes except snowmelt-rainfall ones: drought duration decreases on average by 25 days and volume deficit by 47%. This signal is less visible for composite 1 and snowmelt-rainfall 2 regimes, but is confirmed by the regional analysis for composite 1 regimes in the northwest region, and snowmelt-rainfall 2 regimes in the southeast region. Conversely, snowmelt-rainfall 1 regimes present an opposite trend toward more severe winter droughts with volume deficit increasing by 10%.

4.2.2. Timing

Trends in timing indices are scarce, with the exception of the drought end (Fig. 7f), which tends to occur earlier for 21% of stations (Table 2) by 8 days on average overall. However, this trend is particularly marked for glacial, snowmelt-glacial and snowmelt 1 and 2 regimes, with a timing shift of 15 days on average. Moreover, it is also detected at the scale of hydro-climatic regions for snowmelt 2 and snowmelt 3 regimes (Fig. 8). The opposite trend is found for snowmelt-rainfall 1 and 2 regimes where winter droughts are shifted later in the season by 22 days on average. This result is regionally consistent for the southeast region.

4.3. Spring and summer high flows

4.3.1. Intensity

At-site results do not reveal any generalized change for high flow intensity (Fig. 9a-b). However, glacial regimes show significant trends: both snowmelt volume and annual maximum are significantly increasing for 93% and 47% of the stations (Table 2), with trend magnitudes of 29% and 21% respectively. Regional results (Fig. 10) confirm these observations, with regionally consistent upward trends detected on these indices for glacial regimes. On the other hand, a field-significant decrease of the snowmelt annual maximum by an average magnitude of 16% is found for composite and snowmelt-rainfall regimes, but it is not regionally consistent.

4.3.2. Timing

The snowmelt duration has significantly increased for 49% of the stations (Fig. 9c and Table 2) with a trend magnitude of 19 days, mostly owed to an earlier shift in the snowmelt "start" (Fig. 9d). Glacial regimes show significant trends in the snowmelt onset that occurs earlier, with a small magnitude of 6 days, whereas duration does not significantly increase. On the contrary, snowmelt-glacial, snowmelt 1 to 3 and composite 1 regimes exhibit significant decreasing trends for the snowmelt "start" and "center" indices, with average shifts of 10 and 7 days, and increasing trend for the snowmelt "end" index by 11 days. For these regimes, the snowmelt duration consequently increases with a trend magnitude of 23 days. At the scale of hydro-climatic regions (Fig. 10), the same results are observed particularly for snowmelt 1 to 3 and composite 1 regimes, with a significant increase of the snowmelt duration and an earlier onset of the melting season.

4.4. Analysis of long series over the period 1925-2005

In order to assess the stability of detected trends over different time periods, the at-site analysis is repeated for two 40-year periods: 1925-1964 and 1965-2005. Only 22 series (mapped in Fig. 3) are long enough to cover the extended period 1925-2005, thus precluding an analysis of the regional consistency at the scale of hydro-climatic regions.

Figure 11 shows the results of the at-site trend analysis. Generally, the results over the long period 1925-2005 are similar to the main results observed for the whole dataset over the 1961-2005 period described previously. Overall, lower percentiles are the most impacted by significant decreasing trends, whereas higher percentiles are found significantly increasing for snowmelt-rainfall 1 regimes. For low flow indices, snowmelt regimes show a significant trend toward an earlier drought end, a decrease in drought duration and volume deficit. Furthermore, contrasted changes are observed for the annual minimum. Snowmelt-rainfall 1 regimes show results toward less severe winter drought with a clear increasing signal in the annual minimum. However, the drought “end” is found to be shifted earlier, in contrast to the trends observed over the period 1961-2005. For high flow indices, there is a good agreement between the main analysis over the 1961-2005 period and results from the 22 long stations over the 1925-2005 period: snowmelt timing indices “start” and “center” significantly decrease and snowmelt duration increases significantly except for two stations. Contrasted changes can be observed for the snowmelt “end” and no clear trend is found for the snowmelt annual maximum and volume.

Regarding the influence of the time period, slightly more significant trends are detected over the period 1925-2005 than over the two sub-periods: 1925-1964 and 1965-2005 (among which the 1925-1964 period accounts for more significant changes). The detection of significant trends in opposite directions for the two sub-periods would imply a strong inconsistency and an oscillating behavior of the hydrologic indices. This is rarely observed (Fig. 11), but 7 exceptions were found. Among these 7 cases, 5 are not significant overs the 1925-2005 period. Series with significant trends in only one sub-period are more frequent (26 cases) than series with consistent trends over both sub-periods (7 cases).

A particular behavior can be observed for station DE043, with significant increasing trends for almost all percentiles over the period 1925-1964, and even a contradiction in the sub-periods trends for the snowmelt annual maximum. However, these changes could not be explained by any historical change of the gauging station.

These results suggest that the period of analysis (which has been selected in this paper based on data availability rather than on a particular climate-related assumption) plays an important role in the outcome of the trend analysis. Alpine regimes do not seem to have evolved uniformly over time, which calls for further analysis to further understand the main drivers of hydrologic variability in the Alps.

5. Discussion

5.1. Interpreting the results of trend tests

Meaningful trend detection in climate variables requires a good-quality dataset. For this reason, extensive efforts have been made to use a consistent non-influenced streamflow dataset in the AdaptAlp project. However, spurious trends might also be detected if unrealistic assumptions are made by the test. The detection of a significant trend does not prove beyond doubt that a trend actually exists in the data: firstly because of the error level, secondly because what might be rejected is one of the hypotheses used to build the test rather than the null hypothesis. The main questionable assumption relates to the treatment of autocorrelation. Indeed, the local Mann-Kendall test used in this paper assumes that autocorrelation, if present, follows a simple first-order autoregressive structure (AR(1)). Should the data be affected by a more complex dependence structure (for instance, Long-Term Persistence LTP), spurious trends might be detected unduly. This is a difficult issue that, in our opinion, has no clear solution so far. Indeed, while testing procedures adapted to LTP-data have been developed (Cohn and Lins, 2005; Hamed, 2008), these tests make the assumption that data are either LTP or independent. When applied to data presenting only Short-Term Persistence (STP) (e.g. AR(1)), those tests lose their power to detect a trend because they will blame it on spurious LTP. Quoting Jaruskova (1997): "*if the finite part of a time series is observed, it is impossible to distinguish between a stationary series with the positive dependence between* *the neighbouring observations and a sequence of independent variables with the slowly changing mean*". In other words, for a given time series of observations, one can always build a stationary model with complex LTP dependence structure or a simple STP model with some complex non-stationarity that will fit the data equally well. Therefore, this choice has to be made beforehand (using physical considerations if possible), but one should acknowledge that subsequent results are conditioned to this choice.

Finally, in accordance with the review provided by Hall *et al.* (2014) on the understanding of flood regime changes in Europe, we followed a three-step approach by focusing on: (i) trend analysis of individual time series, (ii) field significance of an ensemble of local stations, and (iii) analysis of consistent regional trends. This threefold strategy helps building confidence in the trend detection and highlights general trends at the scale of hydrologic regimes and hydro-climatic regions. Field significant results were found for all major changes observed. Moreover, they are reinforced by the regional consistency test, which provides information on the spatial consistency of detected trends. The regional consistency test is the most stringent (because trends have to be consistent across the hydro-climatic region to be detected), therefore fewer significant trends are found compared with field-significant results at the scale of hydrologic regimes. Nevertheless, trends that are both regionally consistent and field significant are found in 55%, 54% and 42% of the cases for annual percentiles, low flow and high flow indices, respectively (Fig. 6, Fig. 8 and Fig. 10).

In a few cases, field significance and regional consistency tests do not yield the same conclusion. Two opposite situations are identified:

1. A regionally consistent trend is detected, but field significance is not reached. In this case, it is likely that the trend is too small to be detected by at-site tests, and the number of detections is therefore too small to reach field significance. However, if this

small trend is consistent across the hydro-climatic region, the regional consistency test may be able to detect it because it is much more powerful than at-site tests in this case.

2. Field-significant trends are detected, but they are not regionally consistent. This suggests that trends are numerous but not consistent. This might be partly explained by a non-homogenous region, i.e. catchments within the region may have different behaviors that have been overlooked by the clustering methodology. Another explanation is that rivers of the same region are impacted differently over time and thus evolve in different ways. This highlights the difficulty of catchment classification and construction of homogenous climatic regions in a changing context (Krasovskaia and Gottschalk, 2002).

5.2. Comparison with previous studies and attribution

A coherent picture can be drawn for catchments that are highly influenced by snow and glacier melt, which have evolved more drastically than other hydrologic regime types.

For glacial regimes, changes are more numerous for lower and medium percentiles than for upper percentiles (Table 1), which are still field significant. Similar results have been obtained by Birsan *et al.* (2005) where significant trends were generally observed in low flows. Thus winter droughts are shorter and less severe, and spring and summer base flow increase. Pellicciotti *et al.* (2010) also found significant positive trends in annual streamflow for highly glacierized catchments of the Alps, caused by increasing flows in spring and summer. The study concludes that glaciers are still in a phase of enhanced contribution to the total streamflow of their catchment.

For snowmelt-glacial and snowmelt 1 to 3 regimes, a trend toward less severe winter droughts is found. These results are consistent with previous findings, in particular those of the European-wide analysis of Stahl *et al.* (2010). The winter drought timing is not affected except for the "end" which appears to occur earlier. Similar results were observed by Birsan *et al.* (2005), who showed a general increase in winter runoff for alpine catchments in Switzerland. Snowmelt-induced base flow is increasing for rivers that are highly dependent on snow (snowmelt-glacial, snowmelt 1 regimes), and snowmelt duration is found to increase for all the regime types except snowmelt-rainfall 2. According to Birsan *et al.* (2005), increase in winter and spring streamflow is related to changes in temperature rather than changes in precipitation. The study suggests that temperature increase in winter, spring and summer induces a shift in the freezing level with more liquid precipitation during winter, and an earlier and enhanced melt in spring and summer. These results are also consistent with trends found in other mountainous areas of the world. In particular, the trend toward earlier snowmelt flow was also a key finding of Stewart *et al.* (2005) over western North America.

This clear signal on the evolution of winter low flows and spring-summer high flows tends to disappear as the snowmelt influence loses its predominance over other hydrologic flow components. For composite 1 regimes, results tend to be consistent with previous findings. On the contrary, composite 2 regimes show a different behavior with significant increases in winter drought severity (volume deficit and duration), as well as significant decreases in the snowmelt-induced base flow volume. At the end of the Alpine hydrologic spectrum, snowmelt-rainfall regimes show an overall decrease of all percentiles, particularly in the southeast region for lower percentiles. This overall decrease in the percentiles comes from streamflow decrease during the spring and summer periods as it can be observed in the evolution of seasonal percentiles (results not presented here). These results are consistent with the decreasing trends observed for the southern and eastern borders of the Alps by Stahl *et al.* (2010), and with the decrease of precipitation, particularly during the summer, observed in long time series of this region by the HISTALP study (Auer *et al.*, 2007). Regarding low flows, snowmelt-rainfall regimes tend to be affected by later winter droughts, but show contrasted changes in terms of intensity, with more severe winter droughts for snowmelt-rainfall 1 regimes and less severe droughts for snowmelt-rainfall 2 regimes. Conversely, summer droughts tend to occur earlier for both regimes, whereas summer droughts tend to be more severe for snowmelt-rainfall 2 regimes (results not presented in this paper).

As already mentioned, a number of previous studies have demonstrated the link between the evolutions of hydrologic regimes with observed changes in temperature. While a general increase in temperature is observed in the Alps during the 20th century (e.g. Auer *et al.*, 2007), changes in precipitation patterns appear to be more complex. Moreover, empirical comparisons between streamflow trends and forcing variables like precipitation and temperature are difficult to interpret and possibly misleading for two main reasons. First, the complex filtering role of the catchment makes it difficult to determine the expected streamflow response from a given trend in forcing – in particular, a trend in precipitation or temperature should not be expected to identically match what is detected in streamflow. Second, the evolutions affecting distinct forcing variables might compensate each other. As a rough illustration, increasing temperatures and precipitation might (at least partly and temporarily) compensate each other and create no apparent trend in streamflow (at least at the annual scale). Long-term analysis on the Rhone, the Rhine, the Danube and the Po, performed by Zampieri *et al.* (2015), showed that earlier spring streamflow timings are mostly explained by the change of precipitation seasonality and its increasing liquid proportion in these large catchments. While the question remains open for smaller alpine catchments, it calls for further investigation of the role of forcing variables in streamflow trends using some form of hydrologic modeling (see e.g. Renard *et al.*, 2008; Hundecha and Merz, 2012; Merz *et al.*, 2012), which will be investigated in future work.

6. Conclusion

The objective of this paper was to assess the existence of trends in the hydrologic regime of Alpine rivers. This was carried out using a dataset of 177 daily streamflow series. Local and regional statistical tests were applied to various hydrologic indices describing low, medium and snowmelt-related high flows. The main findings can be summarized as follows:

- **Winter droughts**:
  - Severity tends to decrease for all regimes except snowmelt-rainfall regimes, with drought durations decreasing by an average of 25 days over 1961-2005 and volume deficits decreasing by an average of 47%.
  - For the drought "end" a slight shift is detected toward an earlier occurrence for all regimes except snowmelt-rainfall regimes, with an average trend magnitude of 16 days.
  - Mixed snowmelt-rainfall regimes in the Southeastern Alps (mostly Slovenian stations) show an opposite evolution: seasonality seems to be shifted toward later occurrences, for the drought "start", "center" and "end" by 22 days on average. Severity tends to increase for snowmelt-rainfall 1 regimes with a volume deficit increasing by 10%.
- **Spring and summer high flows**:
  - All regimes show a consistent shift toward an earlier start of snowmelt flow, with a trend magnitude of 11 days, along with an increase of 18 days in the duration of the snowmelt season.
  - Glacial regimes, in particular, show a consistent behavior with a melting season shifted by a week earlier, and an increase of 29% in the snowmelt volume and of 21% in the snowmelt induced base flow maximum.

- **Medium flows**:
    - Glacial regimes show a consistent increase in the annual median flow (*Q50*), indicating an enhanced contribution of the glacier to the total streamflow of corresponding catchments.

These results constitute a valuable step toward an improved understanding of the temporal evolution of Alpine hydrologic regimes. In particular, the fact that the trends described above are spatially consistent is an indication that they are climate-related rather than the consequence of measurement issues or direct anthropogenic influences. However, whether these evolutions are linked to climate change or to climate decadal variability remains an open question, which cannot be answered on the sole ground of the analyses described in this paper. Future studies will focus on identifying the role of forcing variables (e.g. precipitation, temperatures) and climate variability (e.g. NAO, ENSO) on the evolution of Alpine hydrologic regimes.

7. Acknowledgements

We would like to thank all data owners for providing the hydrologic data used in this study: Bundesministerium für Land und Forstwirtschaft, Umwelt und Wasserwirtschaft (BMLFUW), Hydrographisches Zentralbüro, French Ministry of Ecology, Sustainable Development and Energy, through the HYDRO database, Electricité de France (EDF), Compagnie Nationale du Rhône (CNR), Bayerisches Landesamt für Umwelt (LfU), Landesanstalt für Umwelt, Messungen und Naturschutz Baden-Württemberg (LUBW), Agenzia Regionale per la Protezione Ambientale (ARPA) Piemonte, ARPA Lombardia, ARPA Veneto, ARPA Friuli Venezia Giulia, ARPA Valle d'Aosta, Ufficio Idrografico della Provincia Autonoma di Bolzano-Alto Adige, Environmental Agency of the Republic of Slovenia, and Federal Office for the Environment, Hydrology Division. Ulrich Looser is gratefully acknowledged for assisting us in making part of this dataset available through the global runoff data center (GRDC). This work was co-funded by the European Union Alpine Space Programme as part of the project AdaptAlp.

8. References

Auer, I., Bohm, R., Jurkovic, A., Lipa, W., Orlik, A., Potzmann, R., Schoner, W., Ungersbock, M., Matulla, C., Briffa, K., Jones, P., Efthymiadis, D., Brunetti, M., Nanni, T., Maugeri, M., Mercalli, L., Mestre, O., Moisselin, J.M., Begert, M., Muller-Westermeier, G., Kveton, V., Bochnicek, O., Stastny, P., Lapin, M., Szalai, S., Szentimrey, T., Cegnar, T., Dolinar, M., Gajic-Capka, M., Zaninovic, K., Majstorovic, Z., Nieplova, E., 2007. HISTALP - historical instrumental climatological surface time series of the Greater Alpine Region. Int. J. Climatol., 27(1): 17-46.

Bard, A., Renard, B., Lang, M., 2012. Floods in the Alpine Areas of Europe. In: Kundzewicz, Z.W. (Ed.), Changes in flood risk in Europe. IAHS Press.

Birsan, M.V., Molnar, P., Burlando, P., Pfaundler, M., 2005. Streamflow trends in Switzerland. J. Hydrol., 314(1-4): 312-329.

Brunetti, M., Lentini, G., Maugeri, M., Nanni, T., Auer, I., Böhm, R., Schöner, W., 2009. Climate variability and change in the Greater Alpine Region over the last two centuries based on multi-variable analysis. Int. J. Climatol., 29(15): 2197-2225.

Brunetti, M., Maugeri, M., Nanni, T., Auer, I., Böhm, R., Schöner, W., 2006. Precipitation variability and changes in the greater Alpine region over the 1800 - 2003 period. J. Geophys. Res., 111(D11).

Burn, D.H., Hannaford, J., Hodgkins, G.A., Whitfield, P.H., Thorne, R., Marsh, T., 2012. Reference hydrologic networks II. Using reference hydrologic networks to assess climate-driven changes in streamflow. Hydrological Sciences Journal: 1-15.

Casassa, G., López, P., Pouyaud, B., Escobar, F., 2009. Detection of changes in glacial run-off in alpine basins: examples from North America, the Alps, central Asia and the Andes. Hydrol. Process., 23(1): 31-41.

Castellarin, A., Pistocchi, A., 2012. An analysis of change in alpine annual maximum discharges: implications for the selection of design discharges. Hydrol. Process., 26(10): 1517-1526.

Cohn, T.A., Lins, H.F., 2005. Nature's style: Naturally trendy. Geophys. Res. Lett., 32(23).

Déry, S. J., Stahl, K., Moore, R. D., Whitfield, P. H., Menounos, B., and Burford, J. E. (2009) Detection of runoff timing changes in pluvial, nival, and glacial rivers of western Canada, Water Resour. Res., 45, W04426, doi:10.1029/2008WR006975.

Douglas, E.M., Vogel, R.M., Kroll, C.N., 2000. Trends in floods and low flows in the United States: impact of spatial correlation. J. Hydrol., 240(1-2): 90-105.

Fleig, A.K., Tallaksen, L.M., Hisdal, H., Demuth, S., 2006. A global evaluation of streamflow drought characteristics. Hydrol. Earth Syst. Sci., 10: 535-552.

Frei, C., Schar, C., 2001. Detection probability of trends in rare events: theory and application to heavy precipitation in the alpine region. American Meteorological Society, 14: 1568-1584.

Giuntoli, I., Renard, B., Lang, M., 2012. Floods in France. In: Kundzewicz, Z.W. (Ed.), Changes in flood risk in Europe. IAHS Press.

Giuntoli, I., Renard, B., Vidal, J.P., Bard, A., 2013. Low flows in France and their relationship to large scale climate indices. J. Hydrol., 482: 105-118.

Hall J., Arheimer B., Borga M., Brázdil R., Claps P., Kiss A., Kjeldsen T.R., Kriaučiūnienė J., Kundzewicz Z.W., Lang M., Llasat M.C., Macdonald N., McIntyre N., Mediero L., Merz B., Merz R., Molnar P., Montanari A., Neuhold C., Parajka J., Perdigão R.A.P., Plavcová L., Rogger M., Salinas J.L., Sauquet E., Schär C., Szolgay J., Viglione A., Blöschl G., 2014. Understanding Flood Regime Changes in Europe: A state of the art assessment. HESS, 18, 2735–2772, doi:10.5194/hess-18-2735-2014

Hamed, K.H., 2008. Trend detection in hydrologic data: The Mann–Kendall trend test under the scaling hypothesis. J. Hydrol., 349(3-4): 350-363.

Hamed, K.H., Rao, A.R., 1998. A modified Mann-Kendall trend test for autocorrelated data. J. Hydrol., 204(1-4): 182-196.

Hannaford, J., Marsh, T.J., 2008. High-flow and flood trends in a network of undisturbed catchments in the UK. Int. J. Climatol., 28(10): 1325-1338.

Hannah, D.M., Demuth, S., van Lanen, H.A.J., Looser, U., Prudhomme, C., Rees, G., Stahl, K., Tallaksen, L.M., 2011. Large-scale river flow archives: importance, current status and future needs. Hydrol. Process., 25(7): 1191-1200.

Hodgkins, G.A., Dudley, R.W., 2011. Historical summer base flow and stormflow trends for New England rivers. Water Resour. Res., 47(7): W07528.

Hundecha, Y., Merz, B., 2012. Exploring the relationship between changes in climate and floods using a model-based analysis. Water Resour. Res., 48(4): W04512.

Huss, M., Farinotti, D., Bauder, A., Funk, M., 2008. Modelling runoff from highly glacierized alpine drainage basins in a changing climate. Hydrol. Process., 22(19): 3888-3902.

IPCC, 2013: Climate Change 2013: The Physical Science Basis. Contribution of Working Group I to the Fifth Assessment Report of the Intergovernmental Panel on Climate Change [Stocker, T.F., D. Qin, G.-K. Plattner, M. Tignor, S. K. Allen, J. Boschung, A. Nauels, Y. Xia, V. Bex and P.M. Midgley (eds.)]. Cambridge University Press, Cambridge, United Kingdom and New York, NY, USA.

Jaruskova, D., 1997. Some problems with application of change-point detection methods to environmental data. Environmetrics, 8(5): 469-483.

Kendall, M.G., 1975. Rank correlation methods. Griffin, London, 202 pp.

Koboltschnig, G.R., Schoner, W., 2011. The relevance of glacier melt in the water cycle of the Alps: the example of Austria. Hydrol. Earth Syst. Sci., 15(6): 2039-2048.

Kundzewicz, Z.W., Graczyk, D., Maurer, T., Pinskwar, I., Radziejewski, M., Svensson, C., Szwed, M., 2005. Trend detection in river flow series: 1. Annual maximum flow. Hydrol. Sci. J.-J. Sci. Hydrol., 50(5): 797-810.

Kundzewicz, Z.W., Robson, A.J., 2000. Detecting trend and other changes in hydrological data, Wallingford, UK, 160 pp.

Lang, M., Pobanz, K., Renard, B., Renouf, E., Sauquet, E., 2010. Extrapolation of rating curves by hydraulic modelling, with application to flood frequency analysis. Hydrological sciences Journal., 55(6): 883-898.

Lins, H.F., Slack, J.R., 1999. Streamflow trends in the United States. Geophys. Res. Lett., 26(2): 227-230.

Mann, H.B., 1945. Nonparametric tests against trend. Econometrica, 13: 245-259.

Merz, B., Vorogushyn, S., Uhlemann, S., Delgado, J., Hundecha, Y., 2012. HESS Opinions "More efforts and scientific rigour are needed to attribute trends in flood time series". Hydrol. Earth Syst. Sci. Discuss., 9(1): 1345-1365.

Moberg, A., Jones, P.D., 2005. Trends in indices for extremes in daily temperature and precipitation in central and western Europe, 1901-99. Int. J. Climatol., 25(9): 1149-1171.

Parey, S., Malek, F., Laurent, C., Dacunha-Castelle, D., 2007. Trends and climate evolution: statistical approach for very high temperatures in France. Clim. Change, 81(3): 331-352.

Pellicciotti, F., Bauder, A., Parola, M., 2010. Effect of glaciers on streamflow trends in the Swiss Alps. Water Resour. Res., 46(10): W10522.

Pettitt, A.N., 1979. A non-parametric approach to the change-point problem. Appl. Statist., 28(2): 126–135.

Pujol, N., Neppel, L., Sabatier, R., 2007. Regional tests for trend detection in maximum precipitation series in the French Mediterranean region. Hydrol. Sci. J.-J. Sci. Hydrol., 52(5): 956-973.

Renard, B., Lang, M., Bois, P., Dupeyrat, A., Mestre, O., Niel, H., Sauquet, E., Prudhomme, C., Parey, S., Paquet, E., Neppel, L., Gailhard, J., 2008. Regional methods for trend detection: Assessing field significance and regional consistency. Water Resources Research, 44(8).

Renard, B., 2006. Détection et prise en compte d'éventuels impacts du changement climatique sur les extrêmes hydrologiques en France. Ph.D Thesis Thesis, INPG / Cemagref, Lyon, France, 364 pp.

Sen, P.K., 1968. Estimates of the regression coefficient based on Kendall's tau. Journal of the American Statistical Association, 63: 1379-1389.

Stahl, K., Hisdal, H., Hannaford, J., Tallaksen, L.M., van Lanen, H.A.J., Sauquet, E., Demuth, S., Fendekova, M., Jodar, J., 2010. Streamflow trends in Europe: evidence from a dataset of near-natural catchments. Hydrol. Earth Syst. Sci., 14(12): 2367-2382.

Stewart, I.T., 2009. Changes in snowpack and snowmelt runoff for key mountain regions. Hydrol. Process., 23(1): 78-94.

Stewart, I.T., Cayan, D.R., Dettinger, M.D., 2005. Changes toward earlier streamflow timing across western North America. J. Climate, 18(8): 1136-1155.

Svensson, C., Kundzewicz, Z.W., Maurer, T., 2005. Trend detection in river flow series: 2. Flood and low-flow index series. Hydrol. Sci. J.-J. Sci. Hydrol., 50(5): 811-824.

Tallaksen, L.M., Van Lanen, H.A.J., 2004. Hydrological Drought: processes and estimation methods for streamflow and groundwater. Developments in Water Science. Elsevier, 580 pp.

Viviroli, D., Archer, D.R., Buytaert, W., Fowler, H.J., Greenwood, G.B., Hamlet, A.F., Huang, Y., Koboltschnig, G., Litaor, M.I., López-Moreno, J.I., Lorentz, S., Schädler, B., Schreier, H., Schwaiger, K., Vuille, M., Woods, R., 2011. Climate change and mountain water resources: overview and recommendations for research, management and policy. Hydrol. Earth Syst. Sci., 15(2): 471-504.

Von Storch, H., Navarra, A., 1999. Analysis of Climate Variability: Applications of Statistical Techniques. Springer Verlag, 2nd updated extended edition, 342 pp.

Wehrens, R., Buydens, L.M.C., 2007. Self- and Super-organizing maps in R : the Kohonen Package. Journal of Statistical Software, 21: 1-19.

Whitfield, P. H., 2013. Is 'Centre of Volume' a robust indicator of changes in snowmelt timing? Hydrol. Process., 27: 2691–2698.

Whitfield, P.H., Burn, D.H., Hannaford, J., Higgins, H., Hodgkins, G.A., Marsh, T., Looser, U., 2012. Reference hydrologic networks I. The status and potential future directions of national reference hydrologic networks for detecting trends. Hydrological Sciences Journal: 1-18.

Zamperi, M., Sococcimarro, E., Gualdi, S., Navarra, A., 2015. Observed shift towards earlier spring discharge in the main Alpine rivers. Science of the Total Environment, 503: 222-232

9. Appendix 1. Description of testing procedures.

Throughout this appendix, the random variables representing a series of observations are noted $X_1, ..., X_n$. For regional testing procedures with p stations, the site i is denoted using a superscript, yielding random variables $\left(X_k^{(i)}\right)_{k=1:n, i=1:p}$.

9.1. Modified Mann-Kendall test

The Mann-Kendall statistic S is computed as follows:

$$S = \sum_{i=1}^{n-1} \sum_{j=i+1}^{n} sign(X_j - X_i) \quad (1)$$

The test statistic Z is then defined by:

$$Z = \begin{cases} (S-1)/\sqrt{Var(S)} \text{ if } S > 0 \\ 0 \text{ if } S = 0 \\ (S+1)/\sqrt{Var(S)} \text{ if } S < 0 \end{cases} \quad (2)$$

$$\text{with } \mathrm{Var}(S) = n(n-1)(2n+5)/18$$

This statistic asymptotically follows a Gaussian distribution $N(0;1)$ under the H0 hypothesis of no trend (Mann, 1945; Kendall, 1975).

The variance Var(S) in equation (2) has to be corrected in the following cases:

- In the presence of tied values, the variance is computed as:

$$Var(S) = \left(n(n-1)(2n+5) - \sum_{k=1}^{n} t_k k(k-1)(2k+5) \right) / 18 \quad (3)$$

where t_k is the number of tied values of extent k.

- In the presence of autocorrelation, the variance is computed as (Hamed and Rao, 1998):

$$\mathrm{Var}(S) = \frac{n(n-1)(2n+5)}{18} \times \left[1 + \frac{2}{n(n-1)(n-2)} \sum_{k=1}^{n-1} (n-k)(n-k-1)(n-k-2)\rho_k\right] \qquad (4)$$

where ρ_k is the lag-k autocorrelation coefficient. In this paper, we made the additional assumption of an order-1 autoregressive dependence structure (AR(1)), in order to avoid computing numerous lag-k autocorrelation coefficients with relatively short series. This corresponds to replacing ρ_k by $(\rho_1)^k$ in equation (4).

9.2. Field significance evaluation

Field significance of at-site Mann-Kendall tests is evaluated using the Bootstrap procedure suggested by Douglas *et al.* (2000),

Repeat for $m = 1{:}N_{sim}$, where N_{sim} represents the number of bootstrap replicates:

a) Set $w_m = 0$.

b) Bootstrap the years used in the original data set, yielding a sample $(y_1,\dots,y_n)$.

c) Repeat for $i = 1{:}p$

i) Apply the Mann-Kendall test to the series $X_{y_1}^{(i)},\dots,X_{y_n}^{(i)}$

ii) If the test is significant, increment w_m, $w_m := w_m + 1$

The sample $(w_m)_{m=1:N_{sim}}$ approximates the distribution of the number of significant results amongst p sites, under the H0 hypothesis that all sites are stationary. Field significance is therefore evaluated by comparing the observed number of significant results, w_{obs}, with an empirical quantile computed from $(w_m)_{m=1:N_{sim}}$.

9.3. Regional consistency test

Let $\boldsymbol{X} = \left(X_k^{(i)}\right)_{k=1:n,i=1:p}$ denote the matrix of data, observed at years $(y_1,\dots,y_n)$. We define the following quantities:

- $\tilde{\boldsymbol{X}} = \left(\tilde{X}_k^{(i)}\right)_{k=1:n, i=1:p}$ is the matrix of data transformed by normal score, i.e.:

$$\tilde{X}_k^{(i)} = \phi^{-1}\left(\hat{F}_i\ (X_k^{(i)})\right) \tag{5}$$

where ϕ is the cdf of the standard Gaussian distribution and $\hat{F}_i$ is the empirical cdf of site *i*.

- $\tilde{\boldsymbol{y}} = \left(\tilde{y}_k\right)_{k=1:n}$ is the vector of centered years, i.e. $\tilde{y}_k = y_k - \bar{y}$.
- $\boldsymbol{1}_p$ is a vertical vector of size *p* with all components equal to one.

With this notation, the following value $\hat{\beta}$ is an estimator of a common trend affecting all sites (after transforming data by normal score, see Renard *et al.* (2008)):

$$\hat{\beta} = \frac{\boldsymbol{1}_p^T \left(\tilde{\boldsymbol{X}}^T \tilde{\boldsymbol{X}}\right)^{-1} \tilde{\boldsymbol{X}}^T \tilde{\boldsymbol{y}}}{\tilde{\boldsymbol{y}}^T \tilde{\boldsymbol{y}} \boldsymbol{1}_p^T \left(\tilde{\boldsymbol{X}}^T \tilde{\boldsymbol{X}}\right)^{-1} \boldsymbol{1}_p} \tag{6}$$

The significance of this trend can be assessed using the following deviance statistics, based on a multivariate Gaussian assumption:

$$Z = -2\left(\sum_{k=1}^{n} \log\left(N(X_k^{(1)},...,X_k^{(p)} \mid 0, \hat{\boldsymbol{\Sigma}})\right) - \sum_{k=1}^{n} \log\left(N(X_k^{(1)},...,X_k^{(p)}; \hat{\beta}\tilde{y}_k, \hat{\boldsymbol{\Sigma}})\right)\right) \tag{7}$$

where $N(u^{(1)},...,u^{(p)} \mid \boldsymbol{\mu}, \boldsymbol{\Gamma})$ is the pdf of a *p*-variate Gaussian distribution with mean $\boldsymbol{\mu}$ and variance $\boldsymbol{\Gamma}$, and $\hat{\boldsymbol{\Sigma}}$ is an estimate of the correlation matrix of transformed data $\tilde{\boldsymbol{X}}$, $\hat{\boldsymbol{\Sigma}} = \frac{1}{n}\tilde{\boldsymbol{X}}^T \tilde{\boldsymbol{X}}$. Under the H0 hypothesis of no trend, the deviance statistics *Z* in equation (7) follows a Chi-square distribution with one degree of freedom.

List of captions

Tables

Table 1. Calculation time windows used for the extraction of hydrologic indices.

Table 2. Results of the at-site trend detection. For each regime, numbers give the percentage of downward/upward trends significant at 10% error level. Bold numbers denote field significant trends (with 10% regional error level).

Figures

Figure 1. Summary of the dataset properties. (a) Number of stations per country; (b) distribution of record length; (c) distribution of station elevation; (d) distribution of catchment areas; (e) Evolution of the number of available stations; (f) data availability for each station (colors correspond to Figure 1a).

Figure 2. The nine hydrologic regimes identified for the AdaptAlp dataset. Thin lines represent the inter-annual monthly streamflow of one particular station (after standardization by the inter-annual mean), thick lines represent the within-regime average.

Figure 3. The four HISTALP climatic regions as defined by Auer *et al.* (2007): Northwest (NW), Southwest (SW), Southeast (SE) and Northeast (NE). Symbols represent the classification of the stations in the AdaptAlp dataset into nine hydrologic regimes. The 22 stations with the longest records are marked with inscribed black dots.

Figure 4. Schematic of streamflow indices: (a) low flows; (b) spring and summer high flows.

Figure 5. Results of at-site trend tests (∇ = downward, ▲= upward, x = not significant; blue = downward, red = upward) for percentile indices: (a) Q10, (b) Q25, (c) Q50, (d) Q75, (e) Q90, (f) Q100.

ACCEPTED MANUSCRIPT

Figure 6. Results of the regional test for percentile indices. Rows represent percentile indices, columns represent hydrologic regimes. Each regime is divided into four squares representing the four HISTALP climatic regions (NW, SW, SE and NE), thereby representing hydro-climatic regions. Grey square = non-significant regional trend, red square = significant upward regional trend, blue square = significant downward regional trend, white square = no station for this climate/regime combination. ▲= at-site upward trends are field significant, ▼ = at-site downward trends are field significant, O = at-site trends are not field significant. The number of stations available for each hydro-climatic region is listed in the first row.

Figure 7. Results of at-site trend tests (∇ = downward, ▲= upward, x = not significant; blue = downward, red = upward) for low flow: (a) volume deficit, (b) annual minimum, (c) drought duration, (d) drought “start”, (e) drought “center”, (f) drought “end”.

Figure 8. Same as Figure 6 for low flows.

Figure 9. Results of at-site trend tests (∇ = downward, ▲= upward, x = not significant; blue = downward, red = upward) for high flow : (a) snowmelt volume, (b) snowmelt annual maximum, (c) snowmelt duration, (d) high flow “start”, (e) high flow “center”, (f) high flow “end”.

Figure 10. Same as Figure 6 for high flows.

Figure 11. Stability of detected trends for 22 long series over the period 1925-1965 and over two distinct sub-periods: 1925-1964, 1965-2005.

Table 1. Calculation time windows used for the extraction of hydrologic indices.

Hydrologic Regime	Flow duration percentile			
All hydrologic regime types	1st Dec. – 30th Nov.			
	High Flows		**Low Flows**	
Glacial, snowmelt glacial, snowmelt 1 to 3	1st Feb. – 31st Jan.		1st Jun. – 31st May	
Composite 1 & 2	1st Jan. – 31st Dec.		1st May – 30th Apr.	
	Spring High Flows	**Autumn High Flows**	**Summer Low Flows**	**Winter Low Flows**
Snowmelt rainfall 1 & 2	1st Jan. – 31st Jul.	1st Aug. – 31st Dec.	1st May – 31st Oct.	1st Nov. – 30th Apr.

Table 2. Results of the at-site trend detection. For each regime, numbers give the percentage of downward/upward trends significant at 10% error level. Bold numbers denote field significant trends (with 10% regional error level).

	All		Glacial		Snowmelt glacial		Snowmelt 1		Snowmelt 2		Snowmelt 3		Composite 1		Composite 2		Snowmelt rainfall 1		Snowmelt rainfall 2	
Percentile Indices (number of stations)	*126*		*13*		*5*		*8*		*24*		*17*		*23*		*12*		*6*		*18*	
	down	up	down	up	down	up	down	up	down	up	down	up	down	up	down	up	down	up	down	up
Q10	7	**25**	0	**62**	0	**60**	0	**38**	0	**33**	0	18	9	**22**	8	17	**33**	0	**22**	0
Q25	8	**24**	0	**62**	0	**80**	0	13	0	**21**	0	**29**	13	17	17	**25**	17	0	**22**	0
Q50	8	13	0	**77**	0	20	0	13	0	4	0	6	9	4	**25**	17	0	0	**28**	0
Q75	12	10	0	**77**	0	0	13	0	8	0	18	0	0	4	8	8	**67**	0	**22**	0
Q90	**15**	4	0	**38**	0	0	25	0	8	0	**24**	0	4	0	8	0	**67**	0	**28**	0
Q100	6	13	0	**46**	20	20	13	13	4	8	6	6	0	9	0	0	17	17	17	11
Low Flow Indices (number of stations)	*134*		*13*		*5*		*10*		*25*		*18*		*23*		*12*		*9*		*19*	
	down	up	down	up	down	up	down	up	down	up	down	up	down	up	down	up	down	up	down	up
Start	6	11	0	8	0	20	0	20	8	16	11	0	**17**	4	0	0	0	**33**	0	16
Center	8	7	8	0	20	0	10	0	4	8	17	0	**17**	0	0	0	0	**22**	0	**26**
End	**21**	4	**54**	0	**40**	0	**40**	0	**32**	0	17	0	13	0	8	0	0	**22**	0	**21**
Amin	4	**25**	0	**54**	0	**80**	0	**60**	0	12	0	17	9	**22**	8	8	**22**	0	5	**26**
Duration	**26**	5	**54**	0	**60**	0	**40**	0	**28**	4	**22**	0	17	4	17	**25**	0	11	**21**	5
Volume Deficit	**25**	7	**62**	0	**60**	0	**50**	0	**20**	4	6	0	**17**	9	17	**25**	0	**22**	**26**	5
High Flow Indices (number of stations)	*140*		*15*		*7*		*9*		*29*		*19*		*23*		*12*		*8*		*18*	
	down	up	down	up	down	up	down	up	down	up	down	up	down	up	down	up	down	up	down	up
Start	**49**	1	**33**	0	**29**	0	**44**	0	**100**	0	**42**	0	**26**	0	8	8	**63**	0	**50**	0
Center	**29**	0	**40**	0	**71**	0	**33**	0	**21**	0	**37**	0	4	0	8	0	**38**	0	**50**	0
End	5	**16**	**20**	0	0	**29**	0	**33**	0	**24**	0	**32**	0	9	0	17	13	0	17	6
Amax_baseflow	12	8	0	**47**	0	0	0	11	3	0	0	5	**22**	4	**33**	8	**38**	0	**22**	0
Duration	1	**49**	7	0	0	**43**	0	**89**	0	**90**	0	**58**	0	**57**	0	**25**	0	**50**	0	6
Volume	11	**16**	0	**93**	0	**29**	11	22	3	3	0	0	13	9	**25**	8	13	0	**33**	0

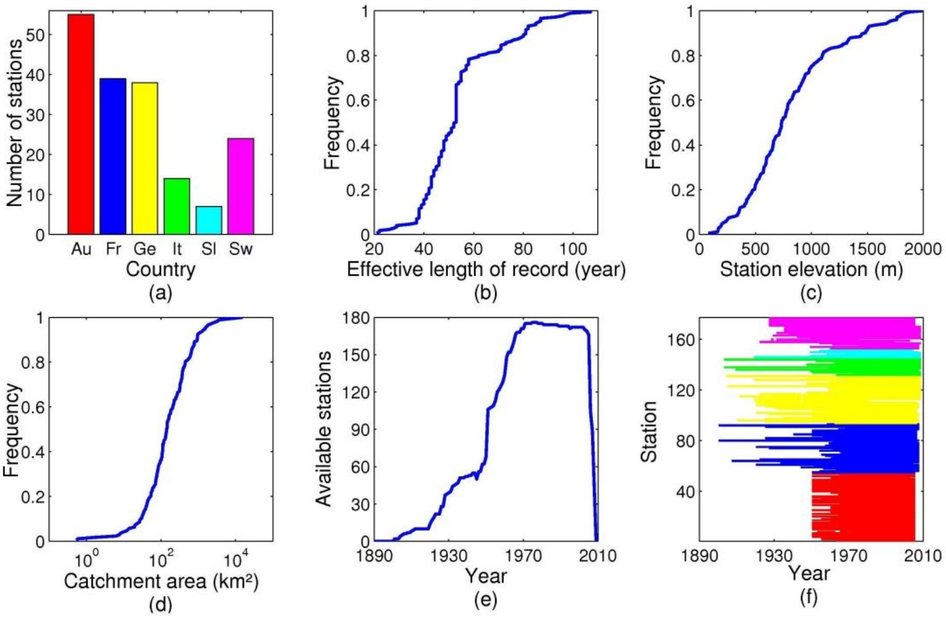

Figure 1. Summary of the dataset properties. (a) Number of stations per country; (b) distribution of record length; (c) distribution of station elevation; (d) distribution of catchment areas; (e) Evolution of the number of available stations; (f) data availability for each station (colors correspond to Figure 1a).

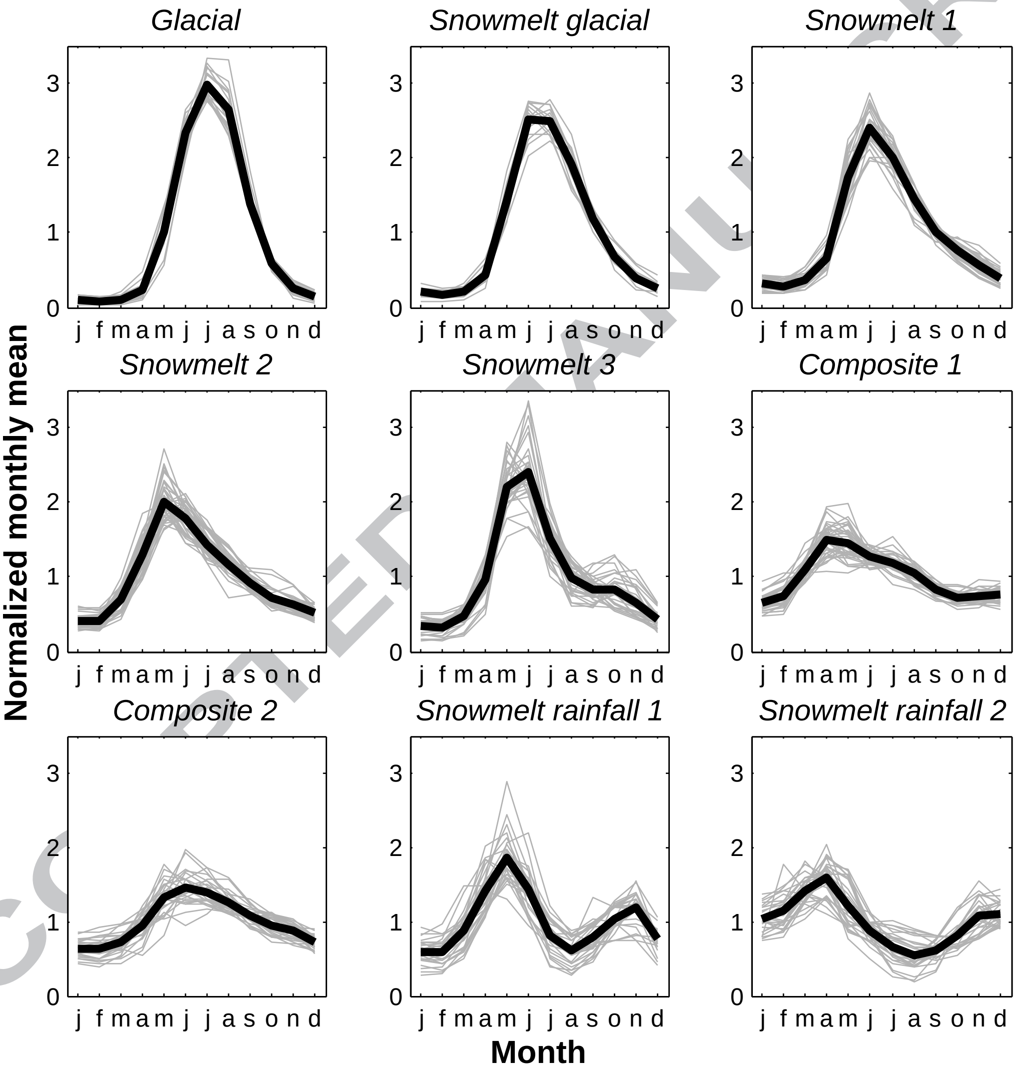

Glacial
Snowmelt glacial
Snowmelt 1
Snowmelt 2
Snowmelt 3
Composite 1
Composite 2
Snowmelt rainfall 1
Snowmelt rainfall 2
Normalized monthly mean
0
1
2
3
j f m a m j j a s o n d
Month

Figure 2. The nine hydrologic regimes identified for the AdaptAlp dataset. Thin lines represent the inter-annual monthly streamflow of one particular station (after standardization by the inter-annual mean), thick lines represent the within-regime average.

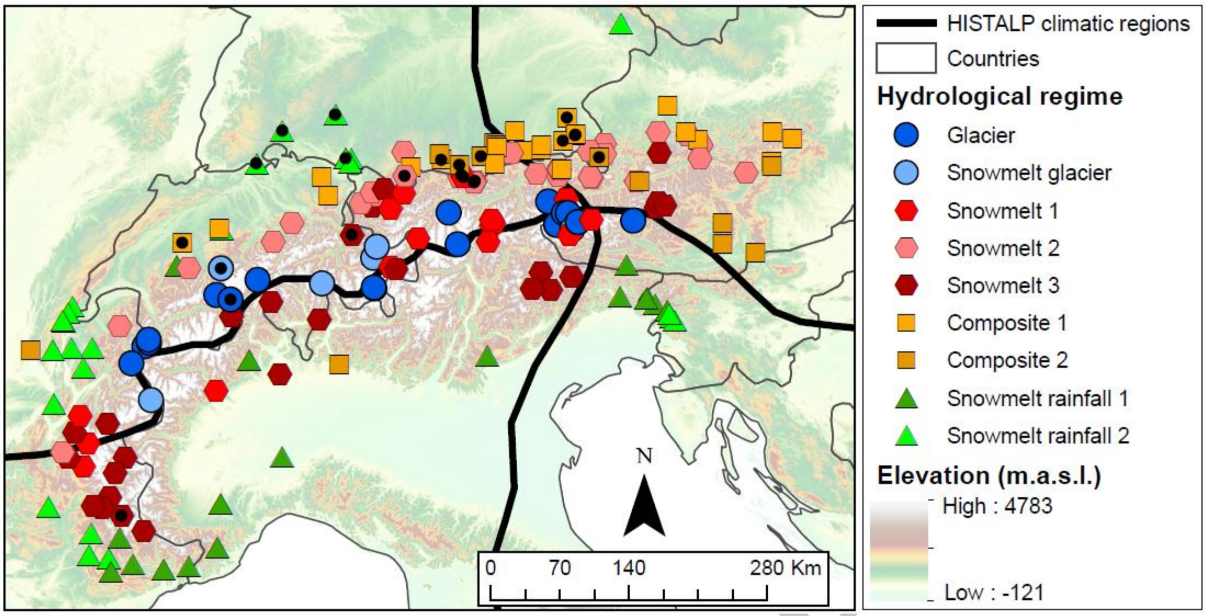

Figure 3. The four HISTALP climatic regions as defined by Auer *et al.* (2007): Northwest (NW), Southwest (SW), Southeast (SE) and Northeast (NE). Symbols represent the classification of the stations in the AdaptAlp dataset into nine hydrologic regimes. The 22 stations with the longest records are marked with inscribed black dots.

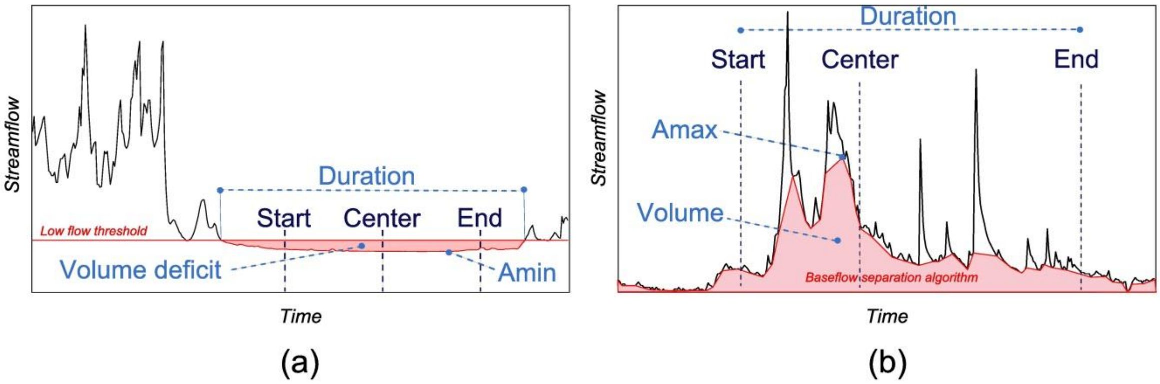

Figure 4. Schematic of streamflow indices: (a) low flows; (b) spring and summer high flows. Timing indices are noted in dark blue, severity indices in light blue.

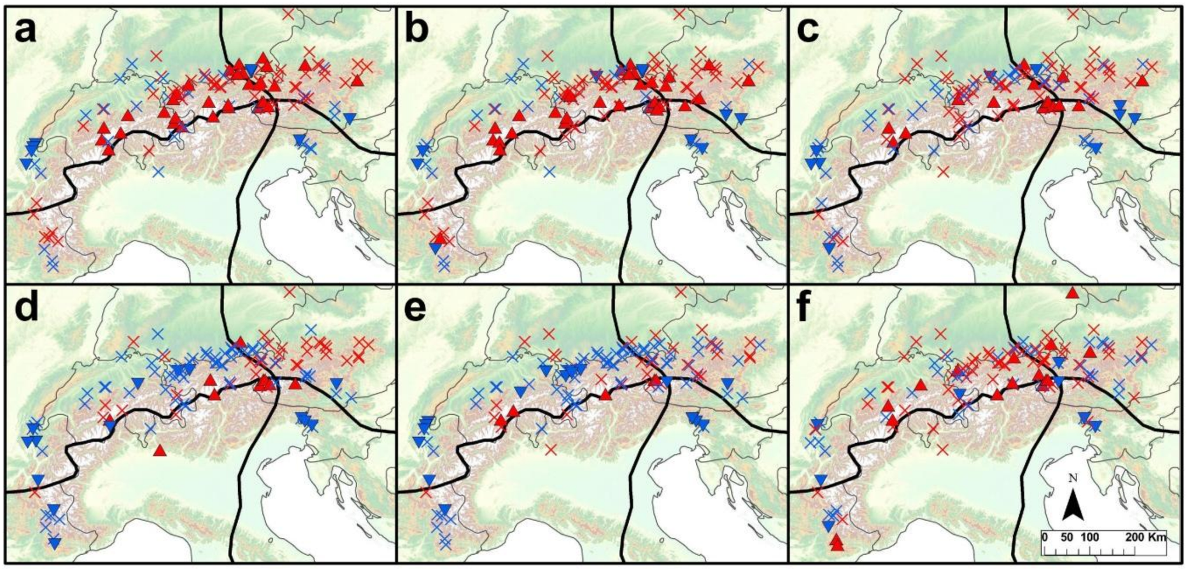

Figure 5. Results of at-site trend tests (∇ = downward, ▲= upward, x = not significant; blue = downward, red = upward) for percentile indices: (a) Q10, (b) Q25, (c) Q50, (d) Q75, (e) Q90, (f) Q100.

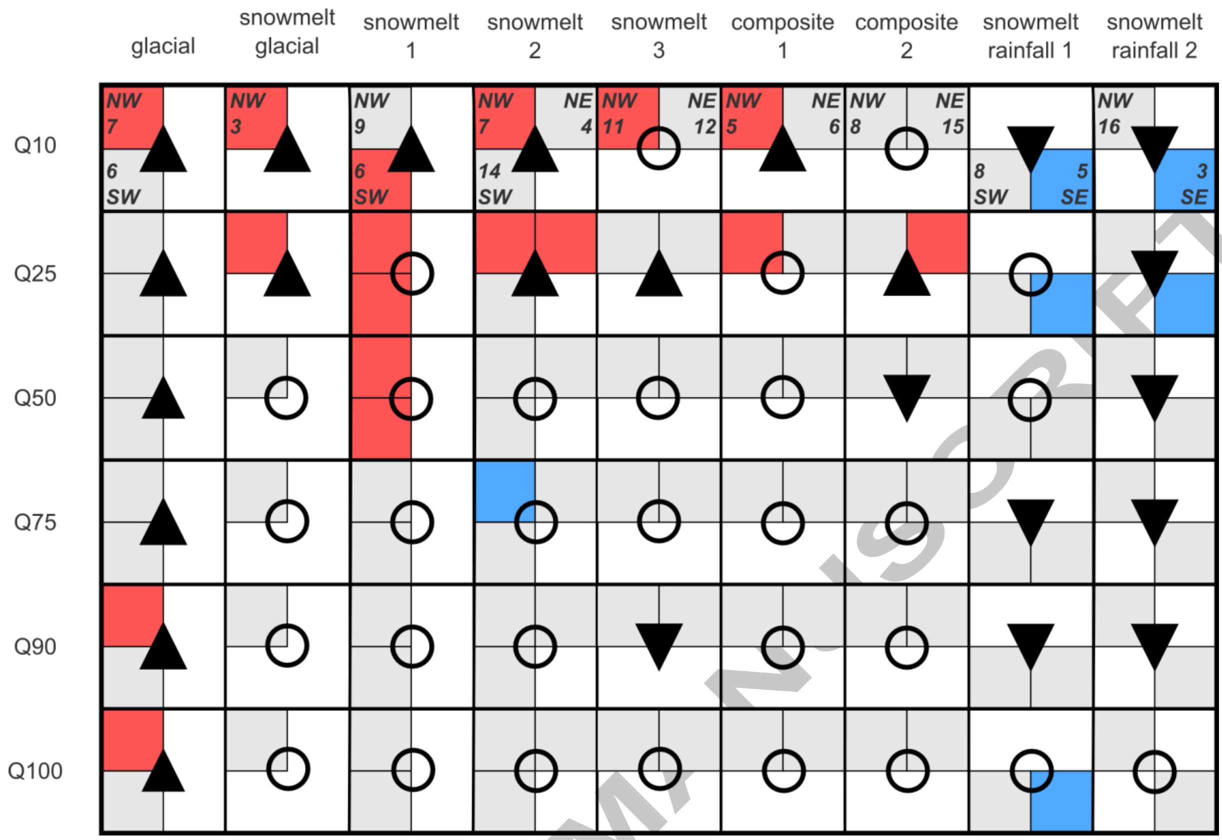

Figure 6. Results of the regional test for percentile indices. Rows represent percentile indices, columns represent hydrologic regimes. Each regime is divided into four squares representing the four HISTALP climatic regions (NW, SW, SE and NE), thereby representing hydro-climatic regions. Grey square = non-significant regional trend, red square = significant upward regional trend, blue square = significant downward regional trend, white square = no station for this climate/regime combination. ▲= at-site upward trends are field significant, ▼ = at-site downward trends are field significant, O = at-site trends are not field significant. The number of stations available for each hydro-climatic region is listed in the first row.

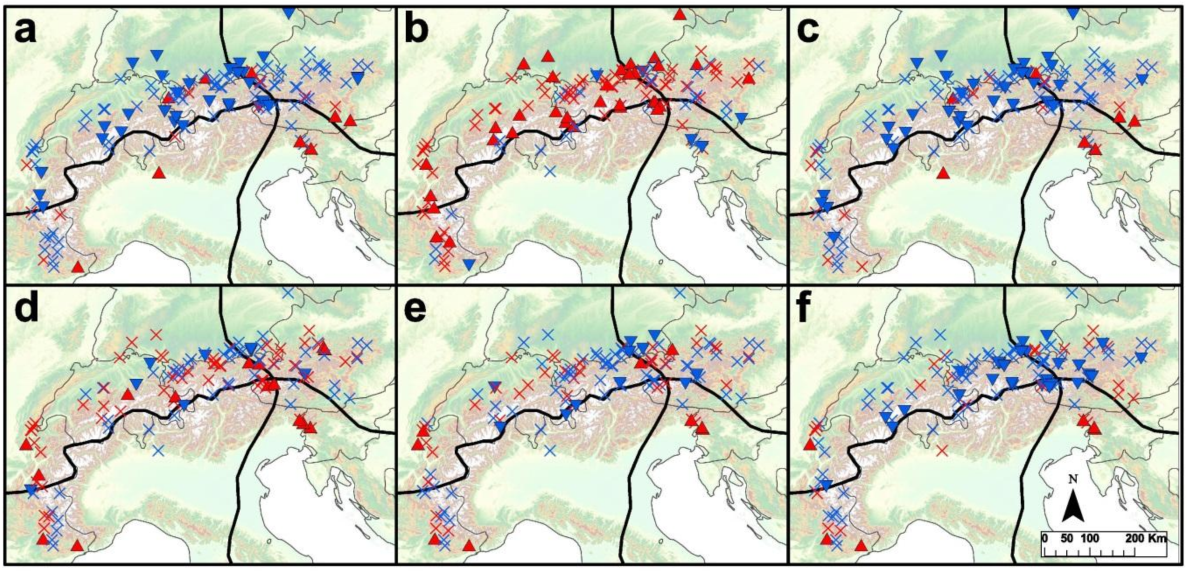

Figure 7. Results of at-site trend tests (∇ = downward, ▲= upward, x = not significant; blue = downward, red = upward) for low flow: (a) volume deficit, (b) annual minimum, (c) drought duration, (d) drought “start”, (e) drought “center”, (f) drought “end”.

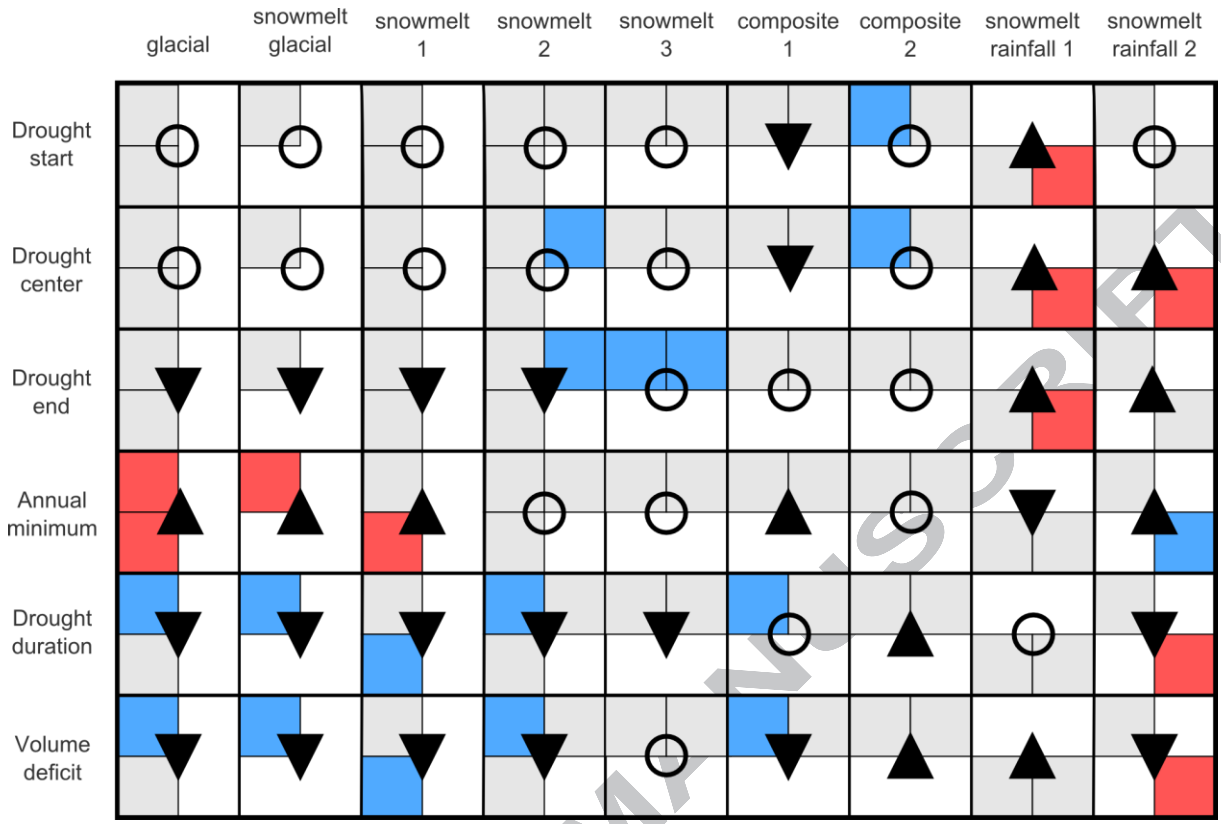

Figure 8. Same as Figure 6 for low flows.

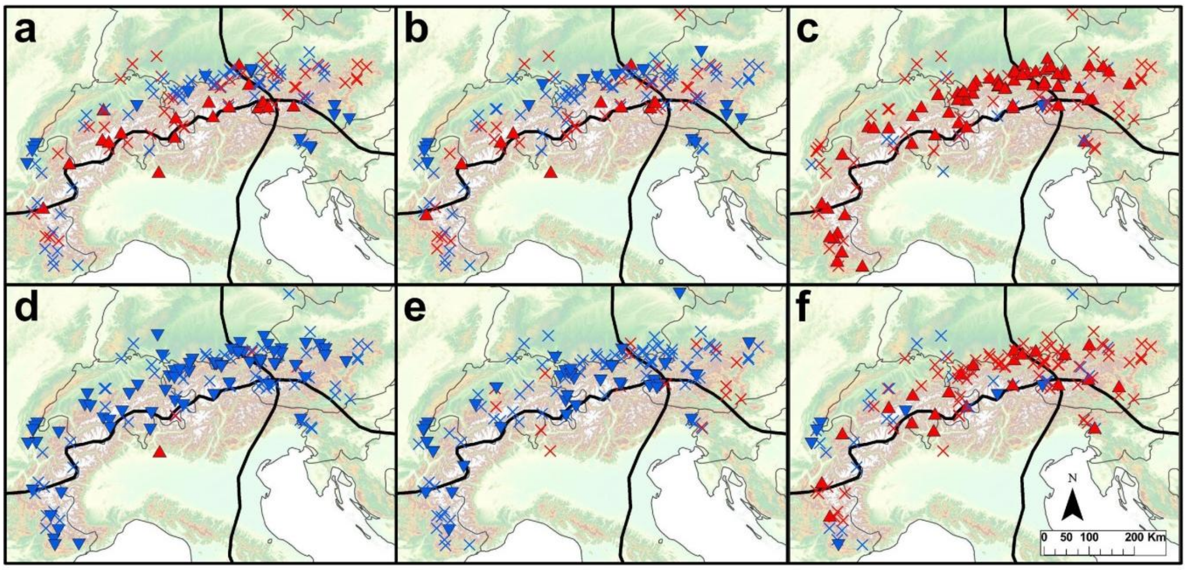

Figure 9. Results of at-site trend tests (∇ = downward, ▲= upward, x = not significant; blue = downward, red = upward) for high flow : (a) snowmelt volume, (b) snowmelt annual maximum, (c) snowmelt duration, (d) high flow "start", (e) high flow "center", (f) high flow "end".

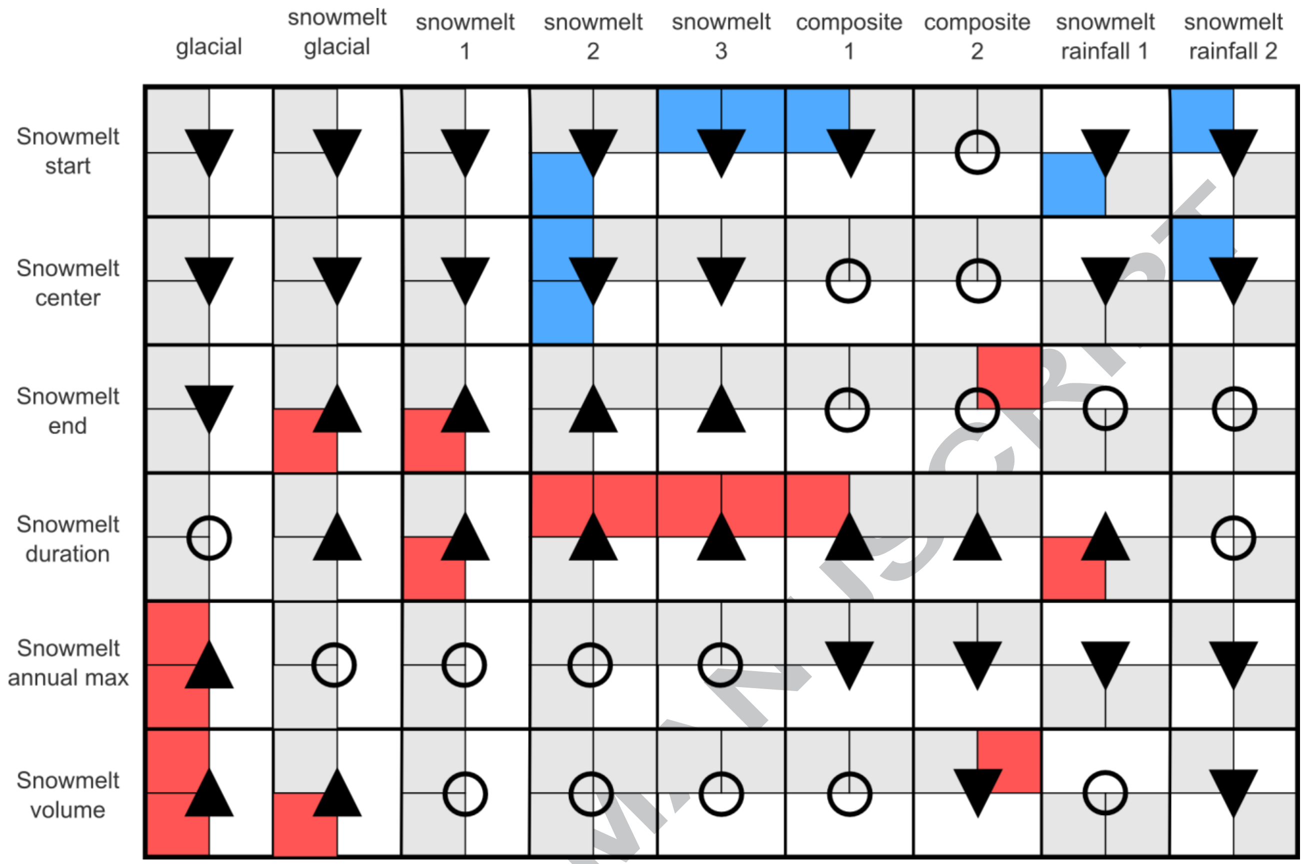

Figure 10. Same as Figure 6 for high flows.

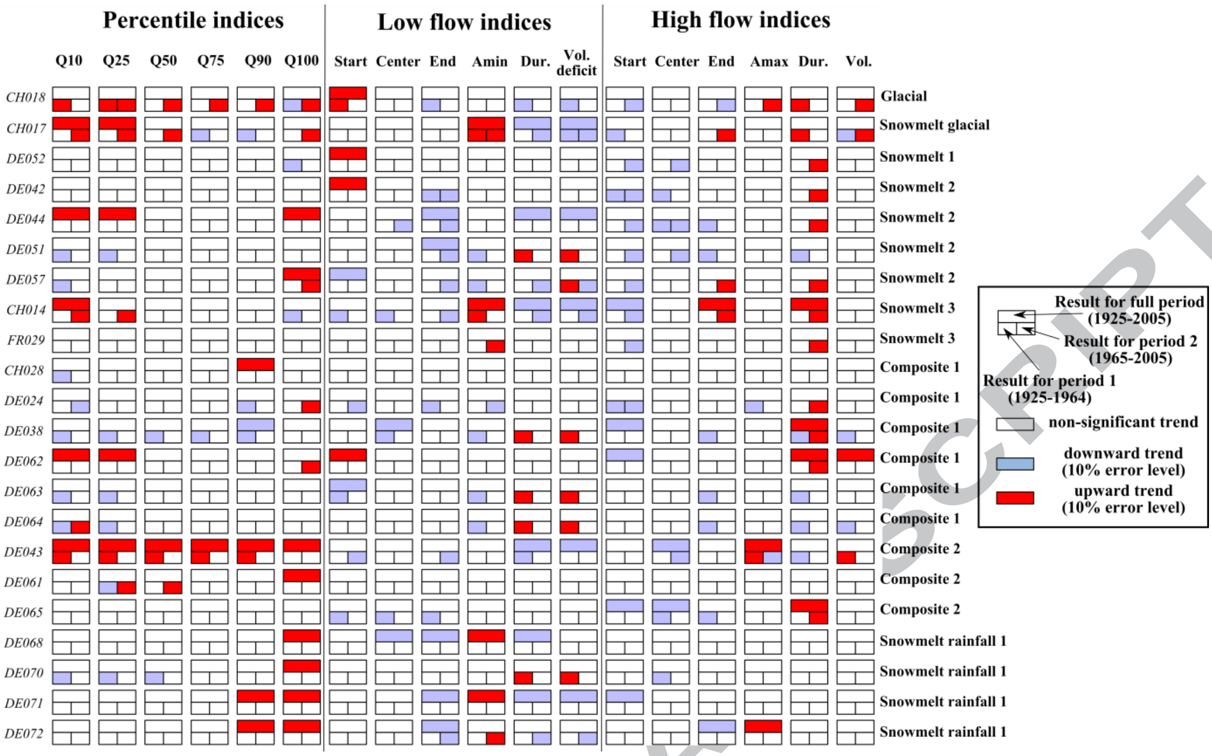

Figure 11. Stability of detected trends for 22 long series over the period 1925-1965 and over two distinct sub-periods: 1925-1964, 1965-2005.

Highlights

- This paper describes a trend analysis of 177 long streamflow series
- Local and regional tests are applied to low, medium and high flow variables
- Less severe winter droughts for most glacier and snowmelt regimes
- Earlier start and increased duration of the snowmelt season for snowmelt regimes
- Glacier regimes show an increase in both mean and peak flows